

Therapeutic targeting of endoplasmic reticulum stress in acute graft-versus-host disease

Eileen Haring,^{1,2,3} Geoffroy Andrieux,^{3,4} Franziska M. Uhl,^{1,2} Máté Krausz,⁵ Michele Proietti,⁵ Barbara Sauer,¹ Philipp R. Esser,⁶ Stefan F. Martin,⁶ Dietmar Pfeifer,¹ Annette Schmitt-Graeff,⁷ Justus Duyster,¹ Natalie Köhler,^{1,8} Bodo Grimbacher,^{5,8,9,10} Melanie Boerries,^{3,4,11} Konrad Aumann,¹² Robert Zeiser^{1,4,8} and Petya Apostolova^{1,3}

¹Department of Medicine I, Medical Center - Faculty of Medicine, University of Freiburg, Freiburg; ²Faculty of Biology, Albert-Ludwigs-University, Freiburg; ³German Cancer Consortium (DKTK), Partner site Freiburg and German Cancer Research Center (DKFZ), Heidelberg; ⁴Institute of Medical Bioinformatics and Systems Medicine, Medical Center - Faculty of Medicine, University of Freiburg, Freiburg; ⁵Institute for Immunodeficiency, Center for Chronic Immunodeficiency (CCI), Medical Center, Faculty of Medicine, Albert-Ludwigs-University, Freiburg; ⁶Allergy Research Group, Department of Dermatology, Medical Center - Faculty of Medicine, University of Freiburg, Freiburg; ⁷University of Freiburg, Freiburg; ⁸CIBSS - Center for Integrative Biological Signalling Studies, University of Freiburg, Freiburg; ⁹DZIF - German Center for Infection Research, Satellite Center Freiburg, Freiburg; ¹⁰RESIST - Cluster of Excellence 2155 to Hannover Medical School, Satellite Center Freiburg, Freiburg; ¹¹Comprehensive Cancer Center Freiburg (CCCF), Medical Center - Faculty of Medicine, University of Freiburg, Freiburg, and ¹²Department of Pathology, Medical Center - University of Freiburg, Faculty of Medicine, University of Freiburg, Freiburg, Germany

Correspondence:

Petya Apostolova
petya.apostolova@uniklinik-freiburg.de

Received: January 17, 2021.

Accepted: August 6, 2021.

Prepublished: August 19, 2021.

<https://doi.org/10.3324/haematol.2021.278387>

©2022 Ferrata Storti Foundation

Haematologica material is published under a CC

BY-NC license 

Therapeutic targeting of endoplasmic reticulum stress in intestinal acute-graft-versus-host disease

Eileen Haring, Geoffroy Andrieux, Franziska M. Uhl, Máté Krausz, Michele Proietti, Barbara Sauer, Philipp R. Esser, Stefan F. Martin, Dietmar Pfeifer, Annette Schmitt-Graeff, Justus Duyster, Natalie Köhler, Bodo Grimbacher, Melanie Boerries, Konrad Aumann, Robert Zeiser and Petya Apostolova

Supplementary files

Contents:

Supplementary Figures	2
Supplementary Tables	10
Supplementary Methods	13

Figure S1 related to Figure 1

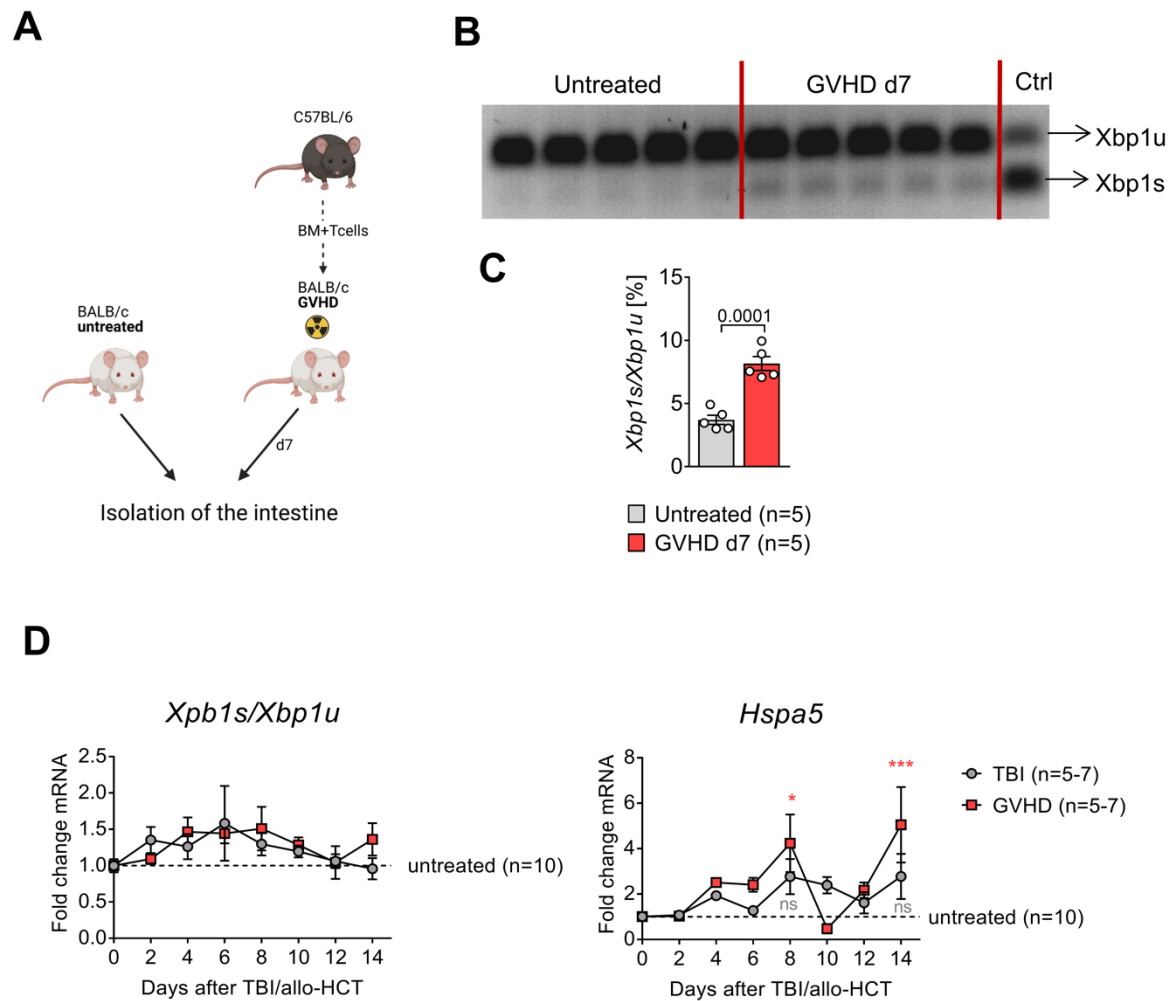


Figure S1. GVHD induction leads to ER stress in the murine intestine

(A) - (C) *Xbp1* splicing assay in untreated mice and mice developing GVHD.

(A) BALB/c mice underwent allo-HCT with 5×10^6 BM cells and 3×10^5 CD4⁺ and CD8⁺ T cells isolated from the spleen of a C57BL/6 donor. Untreated BALB/c mice were used as a control. Schematic overview created with Biorender.com.

(B) Agarose gel electrophoresis result from an *Xbp1* splicing assay performed with colon samples isolated on d7 after allo-HCT. The upper band indicates the unspliced form, the lower band the spliced form of *Xbp1*. Positive control (Ctrl): MODE-K cells treated with 0.2 μ g/ml tunicamycin for 24 h.

(C) Quantification of the ratio of *Xbp1* spliced to unspliced from n=5 mice/group. The *P*-value was calculated using a two-tailed unpaired Student's t-test.

(D) Quantitative real-time PCR analysis of the mRNA expression of selected UPR marker genes in the small intestine with *Actb* as a reference gene. Samples were isolated on different time points after TBI or allo-HCT as described in **Figure 1B**. Data were pooled from two independent experiments with n=10 mice for the untreated group, n=5-7 mice in the TBI and

GVHD groups. The *P*-values were calculated using the ordinary one-way ANOVA with correction for multiple comparisons. Statistical comparisons between “GVHD” and “untreated” are highlighted in red color. Statistical comparisons between “TBI” and “untreated” are highlighted in grey color.

Figure S2 related to Figure 2

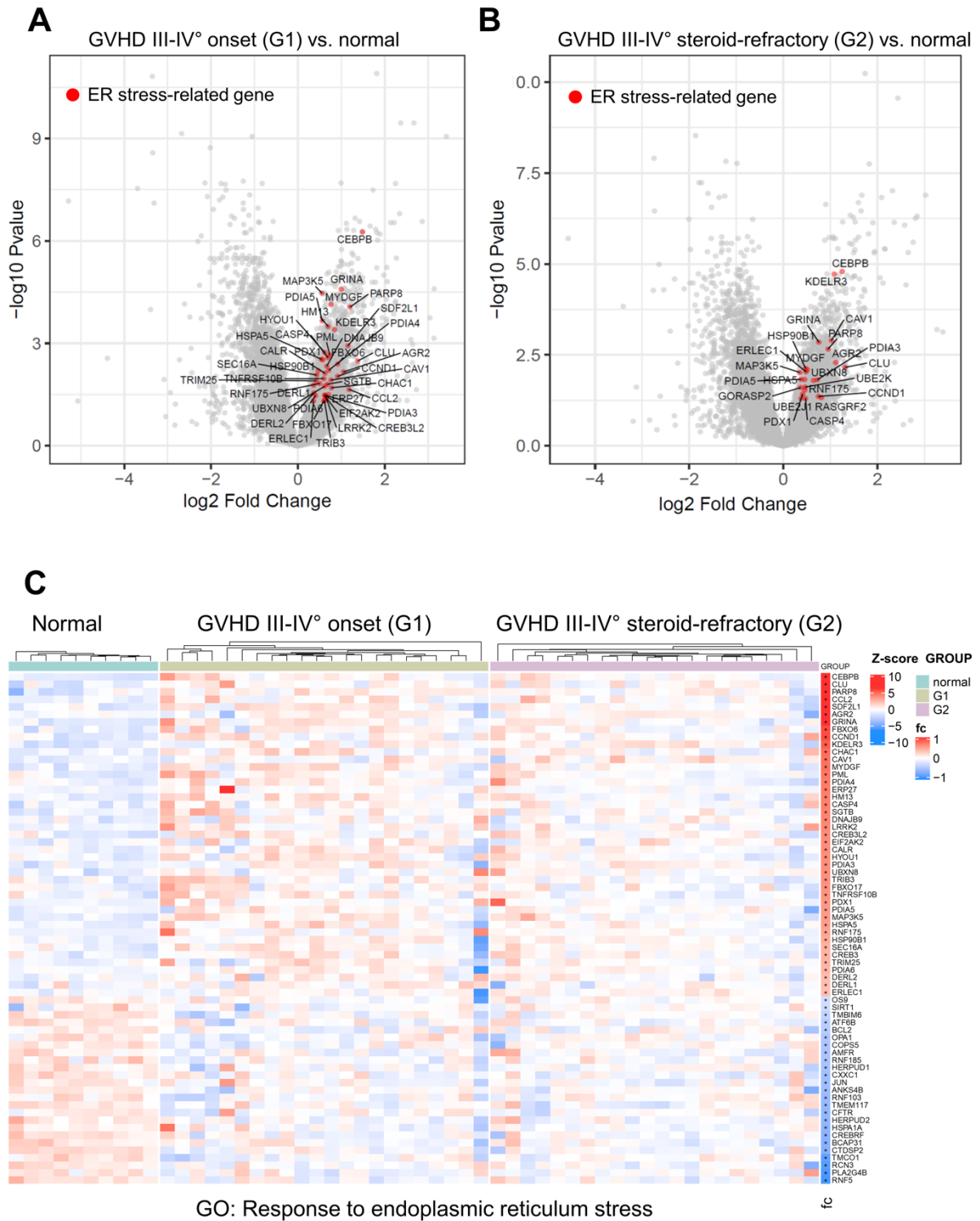


Figure S2. GVHD is associated with a transcriptional signature of increased ER stress in humans

(A) - (C) Analysis of a publicly available RNA sequencing data set (GSE134662)¹.

(A) Volcano plot comparing samples from GVHD III-IV° onset (G1, n=22) with samples from healthy colon tissue (normal, n=10). Red circles highlight genes that are related to ER stress.

(B) Volcano plot comparing samples from patients with steroid-refractory GVHD III-IV° (G2) with samples from healthy colon tissue (normal). Red circles highlight genes that are related to ER stress.

(C) Heatmap for the GO-Term 'Response to endoplasmic reticulum stress' showing expression levels of genes that were differentially expressed between "normal" and "G1". Color legend "Z-score" indicates the row-wise scaling of the normalized intensity, whereas "fc" indicates the log₂ fold change between "G1" and "normal".

Figure S3 related to Figure 3

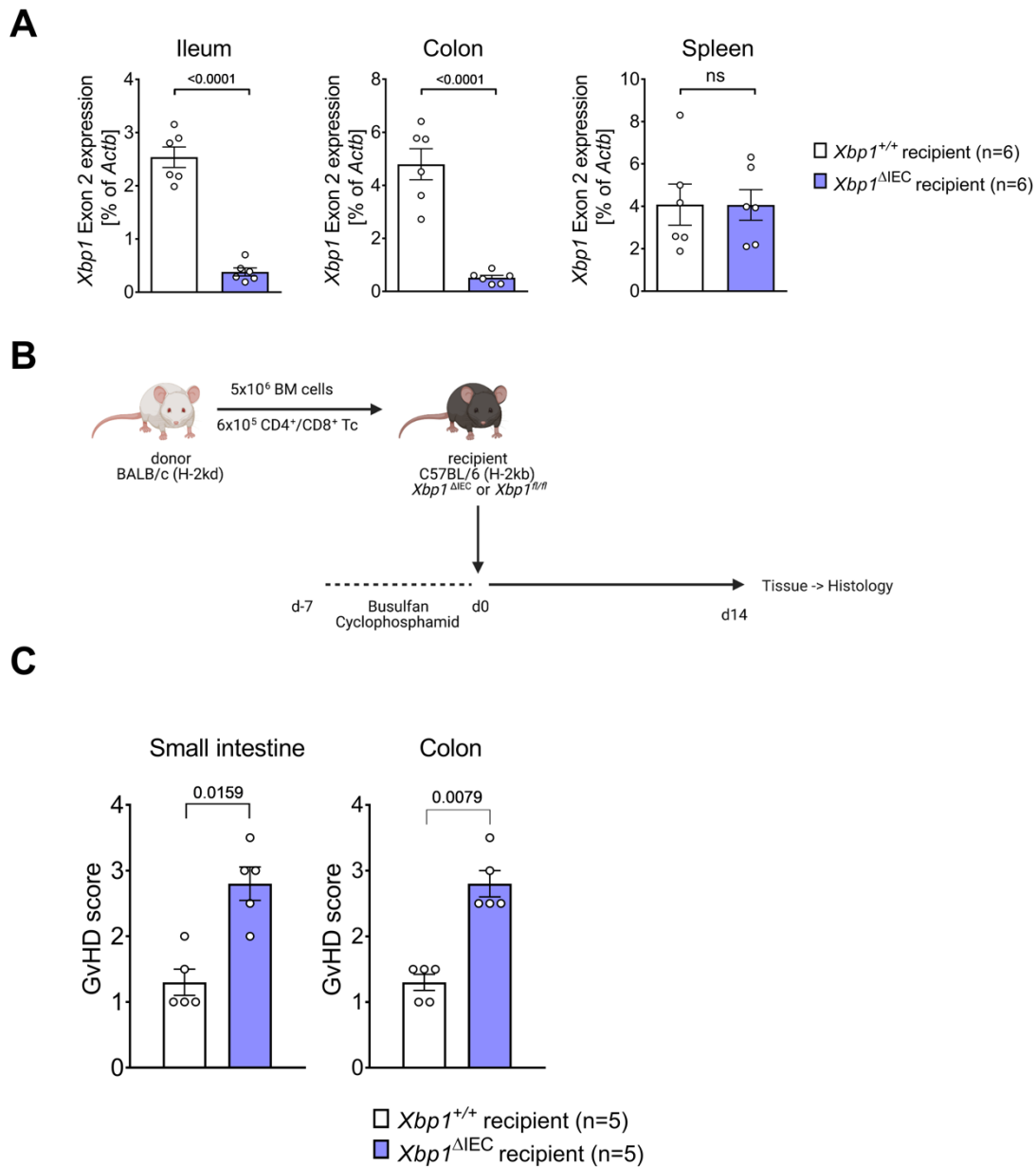


Figure S3. Deletion of intestinal *Xbp1* induces a more severe GVHD phenotype

(A) $Xbp1^{\Delta IEC}$ mice harboring a deletion of exon 2 of the *Xbp1* gene in intestinal epithelial cells were generated as described in Methods. Quantitative real-time PCR analysis of the expression of *Xbp1* exon 2 in the small intestine, colon and spleen in $Xbp1^{\Delta IEC}$ and $Xbp1^{+/+}$ littermates without the Cre-recombinase with *Actb* as a reference gene. Data were pooled from n=6 animals/group. Each dot represents a single mouse. The *P*-values were calculated using the unpaired two-tailed Student's t-test.

(B) Transplantation model with BALB/c (H-2K^d) as donor and *Xbp1*^{ΔIEC} or *Xbp1*^{+/+} as recipients using chemotherapy with busulfan and cyclophosphamide as the conditioning regimen. Schematic overview created with Biorender.com.

(C) Histopathology scores of the small intestine and colon from *Xbp1*^{ΔIEC} and *Xbp1*^{+/+} on d14 after allo-HCT. Data are pooled from n=5 mice/group. Each dot represents a single mouse. The *P*-values were calculated using the unpaired two-tailed Mann Whitney U test.

Figure S4 related to Figure 6

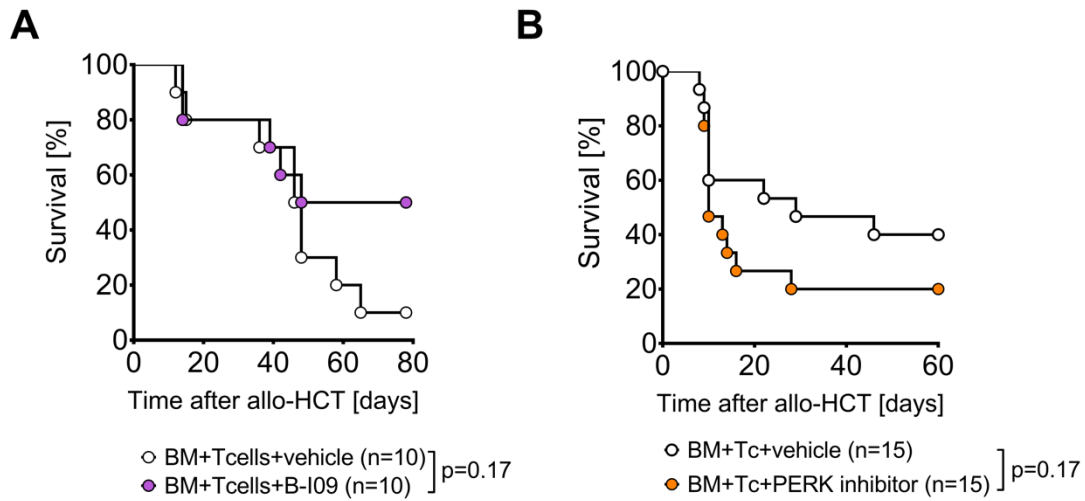


Figure S4. IRE1 α but not PERK inhibition improves GVHD outcome

(A) Survival of BALB/c mice that underwent allo-HCT as described in Figure 6A and were treated with the IRE1 α inhibitor B-I09 for 14 days. Data were pooled from n=10 mice/group. The *P*-value was calculated using the two-sided Mantel Cox test.

(B) Survival of BALB/c mice that underwent allo-HCT as described in Figure 6A and were treated with the PERK-inhibitor GSK2606414 for 7 days. Data were pooled from n=15 mice/group. The *P*-value was calculated using the two-sided Mantel Cox test.

Figure S5 related to Figure 7

A

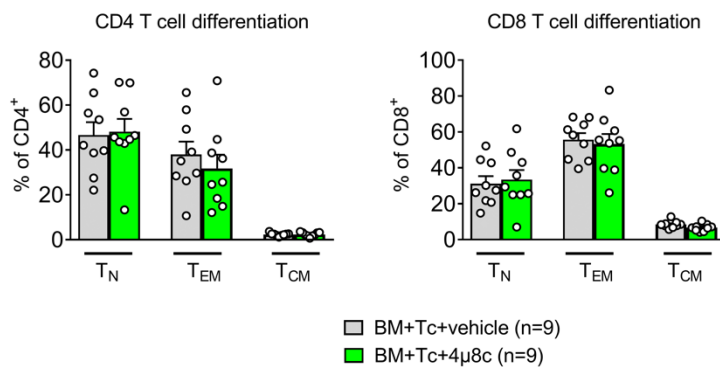


Figure S5. Impact of 4μ8c treatment on systemic immune cell expansion and differentiation

(A) Flow cytometry analysis of peripheral blood T cells isolated from recipient spleens on day 29 after allo-HCT (C57BL/6 in BALB/c model as shown in Figure 7A) and treated with vehicle or 4μ8c (10 mg/kg BW) for 14 days. T cell differentiation into naïve (T_N, CD62L⁺CD44⁻), effector memory (T_{EM}, CD62L⁻CD44⁺) and central memory (T_{CM}, CD62L⁺CD44⁺) T cells is shown. Data were pooled from n=9 mice/group. Each dot represents a single mouse. *P*-values were calculated using the two-tailed unpaired Student's t-test.

Supplementary Tables

Supplementary Table 1. Patient characteristics (immunohistochemical stainings)

Patient number	12 (100%)
Sex	
• Female	5 (42%)
• Male	7 (58%)
Median age (range)	56 (23-78)
Primary disease	
• ALL	2 (17%)
• AML	6 (50%)
• B-NHL	2 (17%)
• Multiple myeloma	1 (8%)
• Primary myelofibrosis	1 (8%)
Donor type	
• Matched unrelated donor	8 (67%)
• Mismatched unrelated donor	2 (17%)
• Matched related donor	2 (17%)
Graft type	
• PBSC	12 (100%)
Conditioning treatment	
• Fludarabin, BCNU, Melphalan	5 (42%)
• Fludarabin, Thiotepa, Melphalan	4 (33%)
• Fludarabin, Thiotepa, Busulfan	1 (8%)
• Fludarabin, Busulfan	1 (8%)
• TBI+Etoposid	1 (8%)
GVHD prophylaxis	
• Cyclosporin A/MMF	8 (67%)
• Cyclosporin A/MMF/ATG	3 (25%)
• Other	1 (8%)
Median day of GVHD onset post allo-HCT (range)	23.5 (9-121)
Intestinal GVHD severity (pathology)	
• Grade 1	2 (17%)
• Grade 2	5 (42%)
• Grade 3	5 (42%)
GVHD treatment	
• Steroids	12 (100%)
• Ruxolitinib	6 (50%)
• Everolimus	1 (8%)
• ECP	1 (8%)

Abbreviations: Allo-HCT: allogeneic hematopoietic cell transplantation, ALL: acute lymphoblastic leukemia, AML: acute myeloid leukemia, ATG: anti-thymocyte globulin, B-NHL: B cell Non-Hodgkin-Lymphoma, ECP: extracorporeal photopheresis, MMF: Mycophenolate mofetil; PBSC: peripheral blood stem cells; TBI: total body irradiation GVHD: graft-versus-host disease.

Supplementary Table 2. Murine qPCR primer

Gene	Primer/Probe	Sequence
<i>Actb</i>	Forward primer	5' CTC AGG AGG AGC AAT GAT CTT GAT 3'
	Reverse primer	5' TAC CAC CAT GTA CCC AGG CA 3'
<i>Bst2</i>	Forward primer	5' CGA GAC ACA GGC AAA CTC CT 3'
	Reverse primer	5' CTC TGG TCA CCG TCT TGT TGT 3'
<i>Ddit3</i>	Forward primer	5' GTC CCT AGC TTG GCT GAC AGA 3'
	Reverse primer	5' TGG AGA GCG AGG GCT TTG 3'
<i>Defa1</i>	Forward primer	5' CTT GTC CTG CTT GGC TTC C 3'
	Reverse primer	5' TTC TCC TGG CTG CTC CTC 3'
<i>Defa4</i>	Forward primer	5' GGC TGT GTC TAT CTC CTT 3'
	Reverse primer	5' TGG TTG TCA TAT CTT TGT CAT 3'
<i>Hspa5</i>	Forward primer	5' TCA TCG GAC GCA CTT GGA A 3'
	Reverse primer	5' CAA CCA CCT TGA ATG GCA AGA 3'
<i>Lamp1</i>	Forward primer	5' TAA CAA CGG AAC CTG CCT GC 3'
	Reverse primer	5' CTC TGG TCA CCG TCT TGT TGT 3'
<i>Lyz</i>	Forward primer	5' GGA TCA ATT GCA CTC TG 3'
	Reverse primer	5' CAG TTC CGA ATA TAC TGG GAC 3'
<i>Reg3g</i>	Forward primer	5' GTA TGA TGC AGA TAT GGC CTG 3'
	Reverse primer	5' ATA TTG GCC ACT GTT ACC AC 3'
<i>Rpn1</i>	Forward primer	5' GAA GCC CAT TCT GGC AAG TG 3'
	Reverse primer	5' GCG CTT GAA CCC GGC G 3'
<i>Xbp1 u</i>	Forward primer	5' GAC AGA GAG TCA AAC TAA CGT GG 3'
	Reverse primer	5' GTA CAG CAG GAC AGA AGG T 3'
<i>Xbp1 s</i>	Forward primer	5' AAG AAC ACG CTT GGG AAT GG 3'
	Reverse primer	5' CTT TTT TGC ACC TGC TGC GGA C 3'
<i>Xbp1 exon 2</i>	Forward primer	5' AGC AGC AAG TGG ATT G 3'
	Reverse primer	5' GAG TTT TCT CCC GTA AAA GCT GA 3'

Supplementary Table 3. Murine *Xbp1* splicing assay primer

Primer/Probe	Sequence
Forward primer	5' ACA CGC TTG GGA ATG GAC AC 3'
Reverse primer	5' CCA TGG GAA GAT GTT CTG GG 3'

Supplementary Table 4. Murine FACS antibodies for extracellular antigens

Antibody	Clone	Company
CD3	17A2	BioLegend
CD4	RM4-5	BioLegend
CD4	V4	BD Pharmingen
CD8	53-6.7	eBioscience
CD8	53-6.7	BD
CD11b	M1/70	eBioscience
CD19	HIB19	BioLegend
CD25	PC61	BioLegend
CD44	IM7	BioLegend
CD45	30-F11	BD
CD62L	MEL-14	BioLegend
CD140a	APA5	BioLegend
CD326	G8.8	BioLegend
H-2kb	AF6-88.5	BioLegend
H-2kd	SF1-1.1	BD
Ly51	BP-1	BD
Ly6G	1A8	Biolegend
UEA-1		Invitrogen

Supplementary Table 5. Murine FACS antibodies for intracellular antigens

Antibody	Clone	Company
CD107a	1D4B	BioLegend
Foxp3	FJK-16s	eBioscience

Supplementary methods

Human subjects

Analysis of the transcriptome in normal colonic biopsies and in GVHD patients was performed using a publicly available RNA sequencing dataset (GSE134662)¹. This data set includes biopsies from 10 healthy controls and 22 patients with GVHD III-IV°. GVHD patient samples were collected at GVHD onset and at a later time point when GVHD was defined as corticosteroid-refractory. Patient data are included in the original publication¹.

Immunohistochemical analysis was performed retrospectively on normal colon biopsies, colitis specimens and samples from GVHD patients recruited at the Medical Center – University of Freiburg. All procedures including human subjects were performed after approval of the local Ethics Committee (250/18) and in accordance with the Declaration of Helsinki. Patient data are included in Supplementary Table 1. This study was registered at Clinicaltrials.gov (NCT04558788).

Chemicals

Recombinant murine TNF was purchased from PeproTech and used at a concentration of 20 ng/ml in cell culture experiments. Tunicamycin (Sigma-Aldrich) was utilized at a final concentration of 1 µg/ml and 0.15 µg/ml respectively in cell culture experiments. IRE1α inhibitor 7-Hydroxy-4-methyl-2-oxo-2H-1-benzopyran-8-carboxaldehyde, 4µ8c, was purchased from Selleckchem and used at a final concentration of 0.2, 1, 2 or 5µM in cell culture experiments and at a concentration of 10 mg/kg body weight in the *in vivo* experiments. B-109 was purchased from MedChemExpress and used at a concentration of 25 mg/kg body weight in the *in vivo* experiments. The PERK inhibitor GSK2606414 was purchased from Axon Medchem and used at a concentration of 20 mg/kg body weight in the *in vivo* experiments.

Allogeneic hematopoietic transplantation and induction of aGVHD

Allo-HCT and induction of aGVHD were performed as described previously². Briefly, recipient BALB/c or C57/BL6 mice received myeloablative conditioning treatment by total body irradiation (TBI) with 10 – 12 Gray (Gy), respectively, in two equal-split doses at least four hours apart. In general, recipient mice were used between 6 and 12 weeks of age and only gender-matched transplantations were performed. In experiments with genetically manipulated recipients, littermates were used as controls. Bone marrow (BM) cells were purified from the femora and tibiae of donor mice whereas CD4⁺ and CD8⁺ T cells were

enriched via positive selection with anti-CD4/CD8 MACS Micro Beads and LS Columns (Miltenyi Biotec) from the spleens. Immediately after the second irradiation, recipient mice received an intravenous injection of 5×10^6 bone marrow (BM) cells and a variable number of CD4⁺ and CD8⁺ T cells depending on the respective transplantation model. For chemotherapy conditioning, the mice received busulfan intraperitoneally (i.p.) at a dose of 20 mg/kg/day from day -7 to day -4, followed by i.p. injection of 100 mg/kg/day cyclophosphamide from day-3 to day-2 prior to allo-HCT. Mice were transplanted on d0 according to the experimental setup.

Bioluminescence imaging

Bioluminescence imaging for luciferase was performed as follows: CD4⁺ and CD8⁺ T cells from a luciferase-transgenic C57BL/6 donor were used for GVHD induction. Recipient mice received an intraperitoneal injection of 150 µg/g body weight luciferin in a total volume of 200 µl PBS. Ten minutes after injection of luciferin, bioluminescence imaging was performed using an IVIS charge-coupled device for 5 minutes. Data acquisition and analysis were performed using the Living Image Software (Xenogen). Light emission was quantified in photons/second/mouse.

Clinical GVHD scoring

Clinical GVHD scoring was performed by two independent investigators according to a recently published system³. This scoring system is based on five clinical parameters: weight loss >10% from baseline, hunching posture, skin lesions, dull fur and diarrhea attested by liquid stool production at time of mice manipulation or its presence in the anal area. Each parameter was scored with 0, if not present, and 1, if present. Dead mice received a total score of 5 until the end of the experiment. The average of the scores from both observers was calculated. Scoring was performed after the signs of irradiation damage had resolved (in our case, starting from day 14 after allo-HCT), and twice per week after that.

Histopathological GVHD grading

To assess the aGVHD histopathology score in mice, small intestine and colon were isolated at indicated time points and fixed in 4% formaldehyde overnight. Following standard dehydration (Leica TP1020 Tissue Processor) and paraffin-embedding procedures (Leica EG1150 Paraffin Embedding Station), 3 µm-thick sections were prepared and stained with hematoxylin/eosin (HE) (Leica AutoStainer XL). AGVHD scoring was performed according to

a previously published scoring system⁴. Intestinal aGVHD was scored on the basis of crypt apoptosis (0, rare to none; 1, occasional apoptotic bodies per 10 crypts; 2, few apoptotic bodies per 10 crypts; 3, the majority of crypts contain an apoptotic body; 4, the majority of crypts contain >1 apoptotic body) and inflammation (0, none; 1, mild; 2, moderate; 3, severe, without ulceration; 4, severe, with ulceration).

AGVHD grading of human intestinal samples was performed using the Lerner scoring system as previously published⁵. Intestinal aGVHD was scored on the basis of crypt apoptosis (I°, isolated single cell apoptosis in crypts without loss of crypts; II°, destruction of single, non-adjacent crypts; III°, loss of several adjacent crypts/ focal mucosal erosions; IV°, excessive loss of crypts in combination with mucosal erosions).

Immunohistochemistry of human and murine intestinal tissue

Intestinal samples were isolated from mice and GVHD patients and fixed in 4% formaldehyde overnight. Following standard dehydration and paraffin-embedding procedures, 2 µm-thick sections were prepared.

For detection of GRP78, the sections were pre-treated in a steamer for 30 minutes at pH 6.1 to enhance epitope retrieval. After washing with PBS and blocking with the Protein Block Serum Free (X909, Dako), human sections were incubated with the anti-GRP78/HSPA5 polyclonal antibody (Sigma, HPA038846) at a dilution of 1:250 in the S3022 medium (Dako) for 1 hour at room temperature. Murine sections were incubated at the same dilution overnight at 4°C. Incubation with the secondary antibody biotin-goat-anti-rabbit E0432 (Dako, dilution 1:400) was performed for 20 minutes at room temperature. For signal detection, the K5005 detection system (Dako) was used. For GRP78 scoring, sections from healthy tissues and from colitis with severe inflammation were stained as a positive and a negative control. Following analysis method was used for evaluating the expression in epithelial cells: epithelium from healthy tissues showed low-intensity signal and were assigned a score of 1; sections from inflamed tissues showed high-intensity signal and were assigned a score of 3. In cases of medium-intensity signal, a score of 2 was assigned.

For detection of CHOP, the sections were pre-treated in Citrate Berlin solution in the microwave at 180 W for 15 minutes to enhance epitope retrieval. After washing with PBS and blocking with the Protein Block Serum Free (X909, Dako), sections were incubated with the anti-GADD153/CHOP antibody, (Novus Biological/NBP2-13172-0) at a dilution of 1:300 in the S3022 medium (Dako) overnight at 4°C. Incubation with the secondary antibody biotin-goat-anti-rabbit E0432 (Dako, dilution 1:400) was performed for 20 minutes at room temperature.

For signal detection, the K5005 detection system (Dako) was used. Scoring for CHOP staining in mouse tissues was performed as follows: ten crypts each from three representative different areas of each section were scored. For each crypt, a score of 0 was assigned, if there were no positive cells, a score of 1, if less than 25% of the cells were positive; 2, if between 25 and 50% of the cells were positive; 3, if more than 50% and up to 75% of the cells were positive; and 4, if more than 75% of the crypt area was positive. The average of each area was determined and the score per section was built as the average of the three areas.

Image acquisition was performed on a Zeiss Axio Imager Z2 using the ZEN software.

Uric acid measurement

Uric acid levels were measured using the Uric Acid Assay Kit (MAK077, Sigma-Aldrich). Organoids were cultured as described and treated with tunicamycin 0.15 µg/ml for 12 h. The next morning, tunicamycin-supplemented medium was carefully washed away and the organoids were allowed to rest for further 24 h in normal, non-supplemented medium. After that, supernatants were removed and directly frozen at -80°C. Measuring uric acid levels was performed using thawed samples, according to the manufacturer's protocols.

RNA isolation and quantitative real-time PCR

RNA was isolated using the miRNeasy Mini Kit from Qiagen following the supplied protocol. For reverse transcription, between 200 and 2000 ng of RNA were utilized and reverse transcription was performed with the High-Capacity RNA-to-cDNA™ Kit (Applied Biosystems, Thermo Fisher Scientific, California, USA) according to the manufacturer's instructions. Gene expression was then quantified using SybrGreen real-time quantitative PCR assays performed on a Roche Light Cycler 480. The Light Cycler 480 Sybr Green I Master kit (Roche) and employed according to the manufacturer's instructions. Primer design was performed using the Beacon Designer software. All primer sequences are listed in Suppl. Table 2. Analysis was performed using the $\Delta\Delta C_t$ method with normalization to *Actb* as a reference gene.

Verification of the successful deletion of exon2 of the *Xbp1* gene was performed utilizing the same method with specific primers as previously described⁶. The primer sequences were published by Kaser et al.⁶ and are listed in Suppl. Table 2.

***Xbp1* splicing assay**

Xbp1 splicing in the intestine was evaluated by gel electrophoresis as previously described⁷. Briefly, cDNA from the intestines of GvHD-developing mice was amplified using primers binding next to the splicing site of *Xbp1*. The unspliced product (171 bp) and the spliced product (145 bp) were separated by agarose gel electrophoresis and visualized under UV light. The primer sequences are listed in Suppl. Table 3. Murine MODE-K cells treated with 0.2 µg/ml tunicamycin for 24 h served as the positive control. Quantification was performed using the Image J software.

Microarray and RNAseq analysis

Microarray analysis of murine small intestine samples was performed using Clariom S Assays (Thermo Fisher Scientific) according to the manufacturer's instructions. CEL files were processed with the oligo R package⁸ and normalized with Robust Multi-array Average (RMA) approach. Relatedness between samples was visualized on a principal component analysis (PCA). Differential expression analysis was performed using a linear model-based approach (limma R package⁹). The significantly regulated genes between *Xbp1*^{ΔIEC} and *Xbp1*^{+/+} were selected with the following criteria: adjusted p value (Benjamini Hochberg procedure) < 0.05. A gene-set enrichment analysis was performed using the GAGE R package¹⁰ comparing *Xbp1*^{ΔIEC} against *Xbp1*^{+/+} (BH adjusted p-value < 0.05) with gene-sets from MSigDB¹¹ and ConsensusPathDB¹². We set the threshold for significant BH-adjusted p-value to 0.05. Differentially regulated genes that belong to relevant gene-sets were visualized as heatmaps or volcano plots. To compare gene expression across the samples we scaled each row using Z-score. Samples and genes were clustered using hierarchical clustering with complete agglomeration method on Euclidean distance. Microarray data are available on GEO under accession number GSE156469 (with the token uhgrqykubhmppl).

RNA sequencing data (FPKM) from the publicly available dataset GSE134662¹ was downloaded at GEO and analyzed as described above for differential gene expression and gene-set enrichment analyses. Regulation of gene expression was visualized as heatmaps or volcano plots

Microbiome analysis

Analysis of the microbiome was carried out as described previously¹³. 16S rRNA data analysis was performed to describe the diversity of bacterial clades in the sample and to provide a rough estimate of their relative abundance. The preprocessing of raw reads was done using the DADA2 pipeline¹⁴ (v.1.14.1) with taxonomic annotation by to Silva reference database¹⁵ (v132). Briefly, the process included the filtering and trimming of the raw reads, followed by sample interference, the stitching together of the paired reads and the removal of chimeric reads. The DADA2 algorithm uses an ASV (amplicon sequence variant) approach¹⁶, which – compared to the OTU (operational taxonomic unit) approach – does not involve clustering of differing sequencing reads. The R package phyloseq was used to import, store and analyze phylogenetic sequencing data and estimate diversity¹⁷. The relative abundance of phyla, classes and families was calculated for each sample as the ratio between the reads for the specific phylum/class/family and the number of total reads for this sample (normalization to sum).

Analysis of peripheral blood

Blood was collected on day 14 and day 29 after allo-HCT and analyzed using a scil Vet abc Plus+ blood analyzer (Horiba) and by flow cytometry.

Thymus digestion

Regeneration of thymic cell populations was analyzed on day 29 after allo-HCT. The thymus was excised, cut in small pieces and enzymatically digested. Briefly, the tissue was incubated twice for 20 minutes in a digestion mix consisting of RPMI supplemented with 25 mM HEPES, 1 mg/ml collagenase D (Roche) and 0.2 mg/ml DNase I (Roche), followed by an incubation step for 20 min in a digestion mix consisting of RPMI supplemented with 25 mM HEPES, 0.0625 mg/ml liberase (Roche) and 0.4 mg/ml DNase I. The digestion solution was filtered through a 70 µm strainer after each digestion step to obtain a single cell solution for flow cytometry staining.

Flow cytometry

Prior to flow cytometry staining, samples were washed with PBS. In general, 200 000 to 500 000 cells were used per staining. Dead cells were marked using the LIVE/DEAD Fixable Aqua Dead Cell Stain Kit (Thermo Fisher Scientific, Germany) or the Red Zombie Fixable Viability

Kit (Biolegend, USA) according to the manufacturer's instructions. Cells were afterwards washed with FACS buffer (PBS supplemented with FCS, EDTA and NaN₃) and Fc block was performed using the purified anti-CD16/CD32 antibody (dilution 1:25, eBioscience-Thermo Fisher Scientific). Antibodies were added at titrated concentrations for 30 minutes. For intracellular stainings, fixation and permeabilization was performed using the BD Cytotfix/Cytoperm kit (BD Biosciences, Germany) or the Foxp3 Fixation/Permeabilization kit (eBioscience, Germany) according to the manufacturer's instructions, followed by incubation with the respective antibodies. After washing, analysis was performed on a BD LSRFortessa Cell Analyzer (BD Biosciences, Germany). All antibodies utilized for flow cytometric analyses can be obtained from Suppl. Tables 4-5. Data were acquired using the BD FACSDiva Software and analyzed with FlowJo_V10.1 (TreeStar, USA). Naïve T cells (T_N) were defined as CD62L⁺ CD44⁻. Effector memory T cells (T_{EM}) were defined as CD62L⁻ CD44⁺. Central memory T cells (T_{CM}) were defined as CD62L⁺ CD44⁺.

Cell culture

The MODE-K cell line, an immortalized mouse intestinal epithelial cell line, was purchased from D. Kaiserlian (INSERM, France) and cultured in RPMI, supplemented with 100 mM sodium pyruvate, 1% HEPES, 1% MEM non-essential Amino Acids, 50 µM 2-mercaptoethanol, 10% fetal calf serum (FCS), 50 U/l penicillin and 50 µg/ml streptomycin¹⁸.

Mouse intestinal organoids were isolated based on the description by Sato and Clevers¹⁹ with adjustments as previously published¹³. Organoid digestion was performed after washing out the Matrigel™ by incubation on a shaking platform in pre-warmed TrypLE Express Enzyme (Gibco-Thermo Fisher Scientific, Germany) for 30 min at 37°C.

Killing assay

Bone marrow-derived dendritic cells were generated from BALB/c mice by flushing out the bone marrow of femur and tibia, lysing the red blood cells and culturing the remaining cells in RPMI, supplemented with 10% FCS, 50 U/ml penicillin, 50 µg/ml streptomycin and 40 ng/ml GM-CSF. Fresh cell culture media and GM-CSF were added on day 3 and 5 of culture. On day 7, mature bone marrow-derived dendritic cells were harvested. CD8⁺ T cells were enriched from the spleen of C57BL/6 mice and co-cultured with dendritic cells at a 5:1 ratio (T cells : dendritic cells) in the presence or absence of 5 µM 4µ8c for 3 days. T cells were harvested after activation and co-incubated with A20 lymphoma cells at different ratios for 24 hours. Killing capacity of CD8⁺ T cells was assessed by flow cytometry.

Statistics

Statistical analysis was performed using the GraphPad Prism Lab Software V7.0 and Microsoft Excel. Comparisons of two groups were carried out by two-tailed unpaired Student's t tests or Mann Whitney U test as indicated. Comparisons of more than two groups were calculated by a one-way ANOVA with correction for multiple testing as appropriate. When data from independent experiments were to be pooled, we set a control group that was consistent among all experiments and normalized the values of all samples as fold change of the control group in order to compensate batch effects. Differences in survival (Kaplan-Meier survival curves) were evaluated using the Mantel Cox (log-rank) test. Analysis of microarray and microbiome data was performed as specified in the respective sections. Data are presented as mean \pm SEM if not indicated otherwise. A *P*-value <0.05 was considered to be significant.

Supplementary References

1. Holtan SG, Shabaneh A, Betts BC, et al. Stress responses, M2 macrophages, and a distinct microbial signature in fatal intestinal acute graft-versus-host disease. *JCI Insight*. 2019;5(17).
2. Tsukamoto H, Chernogorova P, Ayata K, et al. Deficiency of CD73/ecto-5'-nucleotidase in mice enhances acute graft-versus-host disease. *Blood*. 2012;119(19):4554-4564.
3. Naserian S, Leclerc M, Thiolat A, et al. Simple, Reproducible, and Efficient Clinical Grading System for Murine Models of Acute Graft-versus-Host Disease. *Front Immunol*. 2018;9:10.
4. Kaplan DH, Anderson BE, McNiff JM, Jain D, Shlomchik MJ, Shlomchik WD. Target antigens determine graft-versus-host disease phenotype. *J Immunol*. 2004;173(9):5467-5475.
5. Lerner KG, Kao GF, Storb R, Buckner CD, Clift RA, Thomas ED. Histopathology of graft-vs.-host reaction (GvHR) in human recipients of marrow from HL-A-matched sibling donors. *Transplant Proc*. 1974;6(4):367-371.
6. Kaser A, Lee AH, Franke A, et al. XBP1 links ER stress to intestinal inflammation and confers genetic risk for human inflammatory bowel disease. *Cell*. 2008;134(5):743-756.
7. Iwakoshi NN, Lee AH, Vallabhajosyula P, Otipoby KL, Rajewsky K, Glimcher LH. Plasma cell differentiation and the unfolded protein response intersect at the transcription factor XBP-1. *Nat Immunol*. 2003;4(4):321-329.
8. Carvalho BS, Irizarry RA. A framework for oligonucleotide microarray preprocessing. *Bioinformatics*. 2010;26(19):2363-2367.
9. Ritchie ME, Phipson B, Wu D, et al. limma powers differential expression analyses for RNA-sequencing and microarray studies. *Nucleic Acids Res*. 2015;43(7):e47.
10. Luo W, Friedman MS, Shedden K, Hankenson KD, Woolf PJ. GAGE: generally applicable gene set enrichment for pathway analysis. *BMC Bioinformatics*. 2009;10:161.
11. Subramanian A, Tamayo P, Mootha VK, et al. Gene set enrichment analysis: a knowledge-based approach for interpreting genome-wide expression profiles. *Proc Natl Acad Sci U S A*. 2005;102(43):15545-15550.
12. Kamburov A, Stelzl U, Lehrach H, Herwig R. The ConsensusPathDB interaction database: 2013 update. *Nucleic Acids Res*. 2013;41(Database issue):D793-800.
13. Haring E, Uhl FM, Andrieux G, et al. Bile acids regulate intestinal antigen presentation and reduce graft-versus-host disease without impairing the graft-versus-leukemia effect. *Haematologica*. 2021;106(8):2131-2146.
14. Callahan BJ, McMurdie PJ, Rosen MJ, Han AW, Johnson AJ, Holmes SP. DADA2: High-resolution sample inference from Illumina amplicon data. *Nat Methods*. 2016;13(7):581-583.
15. Quast C, Pruesse E, Yilmaz P, et al. The SILVA ribosomal RNA gene database project: improved data processing and web-based tools. *Nucleic Acids Res*. 2013;41(Database issue):D590-596.
16. Callahan BJ, McMurdie PJ, Holmes SP. Exact sequence variants should replace operational taxonomic units in marker-gene data analysis. *ISME J*. 2017;11(12):2639-2643.

17. McMurdie PJ, Holmes S. phyloseq: an R package for reproducible interactive analysis and graphics of microbiome census data. *PLoS One*. 2013;8(4):e61217.
18. Vidal K, Grosjean I, evillard JP, Gespach C, Kaiserlian D. Immortalization of mouse intestinal epithelial cells by the SV40-large T gene. Phenotypic and immune characterization of the MODE-K cell line. *J Immunol Methods*. 1993;166(1):63-73.
19. Sato T, Clevers H. Primary mouse small intestinal epithelial cell cultures. *Methods Mol Biol*. 2013;945(319-328).